Preprints of the 21st IFAC World Congress (Virtual)
Berlin, Germany, July 12-17, 2020

An Adaptive Controller for Robotic Manipulators with Unknown Kinematics and Dynamics

Sihan Wang * **Kaiqiang Zhang** ** **Guido Herrmann** ***

* *Mechanical Engineering Department, University of Bristol, Bristol, BS8 1TR, UK (e-mail: sw16837@my.bristol.ac.uk)*
** *Remote Applications in Challenging Environments, UKAEA, Abingdon,OX14 3DB, UK (e-mail: kaiqiang.zhang@ukaea.uk)*
*** *Department of Electrical & Electronic Engineering, University of Manchester, Manchester, M13 9PL, UK (e-mail: guido.herrmann@manchester.ac.uk)*

Abstract: The ability for kinematics to adapt is important for robotic systems applied in complex environments. This paper focuses on the trajectory control problems of a robotic system with varying kinematics at the end-effector. A new adaptive control approach is developed for robotic manipulators with unknown kinematics and dynamics. This is achieved by using a model-free adaptive controller combined with a kinematics observer. The introduced kinematics observer allows for estimating the kinematic parameters, even under some unconventional application scenarios where typical image processing based techniques are not applicable. Stability of the model-free control with kinematics observer is proven. Control performance and estimation results have been assessed for a wider range of scenarios in a simulation environment which incorporates full nonlinear arm dynamics, finite sampling time and sensor noise.

Keywords: Unknown kinematics, Kinematics estimation, Identification and control methods, Robot manipulators, Adaptive control, Information and sensor fusion.

1. INTRODUCTION

The robotics industry has experienced rapid improvements in productivity and accuracy during the past several decades. However, most application fields are still limited to the industrial uses such as assembly, painting, welding and handling work in the mass-production factories. The working environments of these robots are usually strictly defined, which means the kinematics of these robotic manipulators are fully known. Recently, because of the great advancements in computing performance, novel sensor technology and machine learning, there is an increasing demand of robots in the medical field, service field and even in the household, where the working environment and mission show a high level of diversity. The kinematic adaptability of the manipulator is of great importance in these scenarios. For instance, in waste processing industry (Aitken et al., 2018), a robotic manipulator has to change different tools for classifying, size-reducing and handling objects made of different materials. Therefore, the manipulator must show adaptive performance even when the dimensions of the object or the tool is unknown.

Typical approaches to deal with kinematic uncertainties are based on visual servoing. This concept was firstly published by Shirai et al. (1973), who uses visual information as feedback to reduce the tracking errors of the manipulator. In visual servoing approaches, the control is usually implemented in an image space instead of Cartesian space or joint space, which means it shows great adaptability with unknown robotic kinematics and uncalibrated cameras. For example, Piepmeier et al. (1999) develops a new "dynamic" quasi-Newton strategy. The algorithm successfully addresses the moving target problem for an uncalibrated image-based visual servoing system with 2 degrees of freedom (DOF). Work performed by Hsu et al. (1999), Zergeroglu et al. (2001), Parra-Vega et al. (2003) are limited to the visual servoing control of planar 2 DOF manipulators. Though these results come with different structures or algorithms, all of these controllers require accurate measurement of the end-effector velocity in the image space. This brings significant control inaccuracy. One more degree of freedom is achieved by Wang et al. (2010), who develop a new adaptive controller for image-based tracking of a 3 DOF robot manipulator. Though it does not require accurate image-space velocity measurement, an estimation of the image-space velocity is still required. Visual servoing approach can also be applied to soft robotics, where the deformation of soft components introduces kinematic uncertainties during operations. Navarro-Alarcón et al. (2013) focuses on using a manipulator to realize a deformation controller of an elastic object based on the visual-servoing approach. Satisfying deformation control is successfully obtained without knowing the deformation model of the elastic object or the kinematic parameters of the manipulator kinematics. Nevertheless, the convergence rate of the online estimator is not fast enough for real-time applications at a high motion speed. Therefore, this strategy requires slow motion of the robot manipulators. Wang et al. (2016) applies an adaptive visual servoing controller based on piecewise-constant curvature kinematics to a cable-driven soft manipulator. The controller successfully drives the manipulator to the desired position without knowing the true values of the manipulator's length. However, the convergence rate is relatively slow when the robot is strongly interacting with the environment.

Another common control scheme employs the manipulator's Jacobian matrix for trajectory control without knowing the robot system kinematics. Specifically, work

⋆ The authors would like to acknowledge the support from the EPSRC-funded project Robotics and Artificial Intelligence for Nuclear, (RAIN), EP/R026084/1.

published by Cheah et al. (1999, 2006) present adaptive Jacobian controllers for trajectory tracking of robotic manipulators with uncertain kinematics and dynamics. These algorithms use the measurement of the end-effector position, joint angles and joint velocities to online estimate and update the Jacobian matrix of the manipulator. This control method has been successfully tested on a SONY SCARA robot, which has 2 DOF. In contrast to Cheah's method, Dixon (2007) exploits a feedforward control term that actively compensates for the parametric uncertainty in the Jacobian matrix. One common disadvantage of these control algorithms, based on the estimated Jacobian, is the high complexity of the uncertainty estimators. The regressors in the uncertainty estimators require knowledge of not only joint space position, but also joint space velocity, which greatly increases the computational cost and decreases the estimation accuracy.

In specific industries, the accuracy of the camera measurements heavily depends on the environmental factors, such as brightness (Pérez et al., 2016) or radiation (Aitken et al., 2018). Specifically, in case of radiation, it may not be advisable to mount cameras directly on the manipulator to avoid proximity to a damaging radiation source. A stationary set-up relative to the arm might be more suited to observe the manipulator end-effector. This is the scenario fitting the work in this paper. This paper presents an adaptive control scheme which adapts to the unknown kinematics and the unknown system dynamics of a robot arm. The control scheme consists of a kinematics observer and an adaptive model-free controller. The kinematics observer estimates and updates the unknown parameters online while the only information required is the end-effector position, the joint space position and joint space velocities. In contrast to previous work, the proposed kinematic observer works online where no end-effector velocity is required. This means that it requires no pre-training and low computational power. Moreover, the observer allows for accurate real-time estimations when the kinematic parameters change during manipulator operations.

2. PROBLEM FORMULATION

Here, a typical serial robotic manipulator controlled by motors is considered in this work. This paper assumes that the dynamics (including, link mass, link inertia, and centre of mass position of each robot link) of the system are unknown. This situation is typical in applications using off-the-shelf robots because the detailed designs are confidential or difficult to access. In addition, the unknown objects held by the manipulator introduces dynamic uncertainty. Besides, it is assumed that some kinematics parameters are unknown, since the tool or object held by the manipulator comes with unknown 3D dimensions while the robotic manipulator itself sometimes may come with unknown link length.

As motions of the manipulator are directly provided by the torques generated by each joint motor, the motion equation (Siciliano et al., 2010) of an n-joint robot can be modelled by

$$\tau = M(q)\ddot{q} + V(q,\dot{q})\dot{q} + G(q) \tag{1}$$

where $\tau \in \mathbb{R}^n$ is the vector representing the torque applied at each joint. Vectors $q, \dot{q}, \ddot{q} \in \mathbb{R}^n$ indicate the angular positions, angular velocities and angular accelerations at each joint. $M(q) \in \mathbb{R}^{n\times n}$ is the inertia matrix, $V(q,\dot{q})$ is the vector representing the centrifugal and Coriolis's term, and $G(q)$ denotes the gravity term. Note that the terms M, V and G change with the robot's motions and also vary due to unknown kinematics and dynamics of the system. The dynamics equation shown in Equation (1) is in the joint space q. However, the tasks (like handling) performed by robotic manipulators are usually about to control the robot end effector following a desired trajectory in the Cartesian space. Specifically, the end-effector in this problem is defined as the tip point of the unknown tool held by the manipulator. Though the real-time end-effector position can be measured by a calibrated camera, the real-time end-effector velocity can hardly be measured accurately by a camera. As stated by Wang et al. (2010), since the camera sampling rate is slow in general, the differentiation of camera's imaging output introduces a large noise level of the velocity measurement. Besides, Simoncelli et al. (1991) proved that the accuracy of the velocity measurement is easily affected by the contrast level and camera noise. Therefore, the Cartesian-space end-effector position/velocity are computed from the measurements in joint space with the knowledge of the manipulator kinematics model, shown in the following equations:

$$x = F(q) \qquad \dot{x} = J(q)\dot{q} \tag{2}$$

where x denotes the end-effector position (and orientation) in a 3D Cartesian space. $F(q)$ represents the forward kinematics of the manipulator from its base to the end-effector when holding various tools or objects, $J(q)$ represents the Jacobian matrix of the manipulator. Due to the unknown dimensions of the robot's end-link with an unknown load, both $F(q)$ and $J(q)$ are partially known. This implies similar to Colbaugh et al. (1995), the representation of (1) in the Cartesian space:

$$\tau_c = M_c(q)\cdot\ddot{x} + V_c(x,\dot{x})\dot{x} + G_c(x) \tag{3}$$

In order to follow a desired trajectory, the end-effector is subject to a feedback controller which is designed to minimize the tracking error. The tracking error is defined as:

$$e = x_d - x \tag{4}$$

where x_d represents the demanded end-effector's 3D position in the reference Cartesian space. Therefore, the derivative of the tracking error $\dot{e} = \frac{\partial e}{\partial t}$ with respect to time t can be computed by

$$\dot{e} = \dot{x}_d - \dot{x}. \tag{5}$$

where $\dot{x}_d$ and $\dot{x}$ are the time derivatives of the demand signal x_d and the measurement x in 3D. It can be assumed that x_d and its first two derivatives in time remain bounded.

Here, a calibrated camera is used to identify the tip (end-effector point) of the robot, which may carry an unknown load at the end-effector. The camera measures the Cartesian position of the end-effector point, in order to estimate the 3D dimensional information of the unknown tool via a kinematics observer. One important property is that, the kinematics function (2) can be factorized in terms of a regressor and a vector representing the unknown parameters which are observed:

$$x = Y(q)\Psi \tag{6}$$

where Ψ is the parameter vector (to be estimated) of the kinematics function, and $Y(q) = [Y_{i,j}(q)]$ is the regressor matrix which is a function of joint-space position q.

Subsequently, it is also necessary that $Y(q)$ is persistently excited (Sastry et al., 2011):

$$\int_t^{t+T} Y^T(q)Y(q)dt \geq \epsilon I \tag{7}$$

satisfying the existence of a positive constant ϵ for a specific value of $T > 0$ and all time $t \geq 0$. The kinematics observer designed in this work (discussed in the following section) requires these properties.

3. NOVEL ADAPTIVE CONTROL AND KINEMATICS OBSERVATION SCHEME

3.1 Colbaugh et al.'s Model-free Adaptive Controller

The model-free adaptive controller of Colbaugh et al. (1995) is adopted as a part of the overall adaptive control scheme. The controller is implemented in Cartesian space instead of joint space. Therefore, the required knowledge is the forward kinematics $F(q)$, the end-effector velocity and the Jacobian matrix $J(q)$, for which the kinematics observer and the joint space positions/velocities will be used to estimate those. However, this is still a reduced set of feedback signals and greatly reduces the computational cost (e.g. the inverse kinematics $F^{-1}(q)$ is not required to be computed in real-time).

Firstly, a "modified demanded velocity" and a "weighted position/velocity error" are defined as

$$\dot{x}_d^* = \dot{x}_d + \lambda e \tag{8}$$

$$e^* = \dot{e} + \lambda e = \dot{x}_d^* - \dot{x} \tag{9}$$

where $\dot{x}_d^*$ is the modified demanded velocity, e^* is the weighted position/velocity error, x_d is the desired position in Cartesian space. λ is a positive constant weighting factor to compose the "modified errors". The adaptive control signal is defined as:

$$\tau_A = A(t)\ddot{x}_d^* + B(t)\dot{x}_d^* + f(t) + [2k + K(t)]e^* \tag{10}$$

$$\dot{f} = -\alpha_1 f + \beta_1 e^* \tag{11}$$

$$\dot{A} = -\alpha_2 A + \beta_2 e^* (\ddot{x}_d^*)^T \tag{12}$$

$$\dot{B} = -\alpha_3 B + \beta_3 e^* (\dot{x}_d^*)^T \tag{13}$$

$$\dot{K} = -\alpha_4 K + \beta_4 e^* (e^*)^T \tag{14}$$

where $\tau_A \in \mathbb{R}^n$ is vector of virtual control forces to be applied to τ_c, i.e. $\tau_c = \tau_A$ (3). $k, \alpha_{i=1,2,3,4}$ and $\beta_{i=1,2,3,4}$ are constant positive scalars. $A(t), B(t), K(t)$ and $f(t)$ are time-variable adaptive gains which are updated online. It can be seen in Equations (8) and (9) that, this adaptive controller requires real-time values of the end-effector position and velocity. As the angular measurements q of a robotic manipulator usually take place at each joint by the motor encoders, the most accurate and convenient approach is to measure the manipulator joint space position/velocity. As a result, the end-effector's position and velocity can be computed using the forward kinematics $F(q)$ and Jacobian matrix $J(q)$ online. However, $F(q)$ and $J(q)$ are not fully known due to the unknown tool/load dimensions held by the manipulator. In order to deal with these kinematic uncertainties, a kinematics observer is introduced in the control scheme, which is presented in the following section.

3.2 Unknown Kinematics Observer

The kinematics observer in this scheme is to estimate the unknown 3D dimensions of the end-effector online. The observer requires the real-time measure of the end-effector's position from the camera. The estimation will then be used to update the estimates of $F(q)$ and $J(q)$, which can be used by the model-free adaptive controller.

Firstly, an estimation error e' is defined as the difference between the measured end-effector position x_{pos} (e.g. camera) and the estimated end-effector position:

$$e' = x_{observed} - \hat{F}(q) \tag{15}$$

where $x_{observed}$ is the Cartesian position of the end-effector point measured by the camera and $\hat{F}(q)$ is the estimated end-effector position according to the estimated forward kinematics. The estimation of $\hat{F}(q)$ is defined as:

$$\hat{F}(q) = \hat{x} = Y(q)\hat{\Psi} \tag{16}$$

where $Y(q) = [Y_{ij}(q)]$ is the regression matrix defined in Equation 6 and $\hat{\Psi}$ is the estimated tool dimension parameter vector. This also implies the velocity estimate $\dot{\hat{x}}$:

$$\dot{\hat{x}} = \dot{Y}(q)\hat{\Psi}, \tag{17}$$

where $\dot{Y}_{ij}(q) = \frac{\partial Y_{ij}(q)}{\partial q}\dot{q}$.
The estimation of the tool dimensions are updated online according to the following update law:

$$\dot{\hat{\Psi}} = Y^T(\cdot)\Lambda e' \tag{18}$$

where $\dot{\hat{\Psi}}$ is the rate of change of the estimated parameters, Λ is a positive definite matrix, Y is the regression matrix defined above and e' is the difference between the real end-effector position and the estimated end-effector position (15). This implies the following result in terms of the kinematics observer:

Lemma 1. Assuming the regressor $Y(q)$ is persistently excited, the camera observation is error free $x = x_{observed}$ and we consider $\Psi = \text{const.}$, then the estimate $\hat{\Psi}$ converges exponentially to the true value Ψ, i.e. $\lim_{t\to\infty} \hat{\Psi} = \Psi$ and

$$V_\Psi = (\hat{\Psi} - \Psi)^T(\hat{\Psi} - \Psi) \tag{19}$$

satisfies

$$\dot{V}_\Psi \leq -\alpha_v V_\Psi,\ V_\Psi \leq e^{-\alpha_v t} V_\Psi(t=0) \tag{20}$$

for some $\alpha_v > 0$. •

Remark 1. Note that the assumption of $\Psi = \text{const.}$ can be slightly relaxed to allow for piecewise constant values of Ψ. In a more general case, $\Psi \neq \text{const.}$, the derivative $\dot{\Psi}$ should be assumed to be bounded which would imply a result of ultimate boundedness for the estimation error $(\hat{\Psi} - \Psi)$. ◦

Proof. Let us choose the Lyapunov function of (19). This implies:

$$\dot{V}_\Psi = -(\hat{\Psi} - \Psi)^T Y^T(q)\Lambda Y(q)(\hat{\Psi} - \Psi) \tag{21}$$

Given persistent excitation of $Y(q)$ (7), Theorem 2.5.1 and 1.5.2 of Sastry et al. (2011) implies exponential convergence of the error $(\hat{\Psi} - \Psi) \to 0$ and (20). ■

3.3 Adaptive Control with Unknown Kinematics Observer

Figure 1 presents how the model-free adaptive controller interacts with the kinematics observer. Hence, the control system with the kinematics observer is summarized as:

$$\hat{e} = x_d - \hat{x}, \qquad \dot{\hat{e}} = \dot{x}_d - \dot{\hat{x}} \tag{22}$$

$$\dot{\hat{x}}_d^* = \dot{x}_d + \lambda\hat{e} \tag{23}$$

$$\hat{e}^* = \dot{\hat{e}} + \lambda\hat{e} = \dot{\hat{x}}_d^* - \dot{\hat{x}} \tag{24}$$

so that the adaptive control law with kinematics observer is to be rewritten as:

$$\tau = A(t)\ddot{x}_d^* + B(t)\dot{\hat{x}}_d^* + f(t) + [2k + K]\hat{e}^* \tag{25}$$

$$\dot{f} = -\alpha_1 f + \beta_1 \hat{e}^* \tag{26}$$

$$\dot{A} = -\alpha_2 A + \beta_2 \hat{e}^* (\ddot{\hat{x}}_d^*)^T \tag{27}$$

$$\dot{B} = -\alpha_3 B + \beta_3 \hat{e}^* (\dot{\hat{x}}_d^*)^T \tag{28}$$

$$\dot{K} = -\alpha_4 K + \beta_4 \hat{e}^* (\hat{e}^*)^T \tag{29}$$

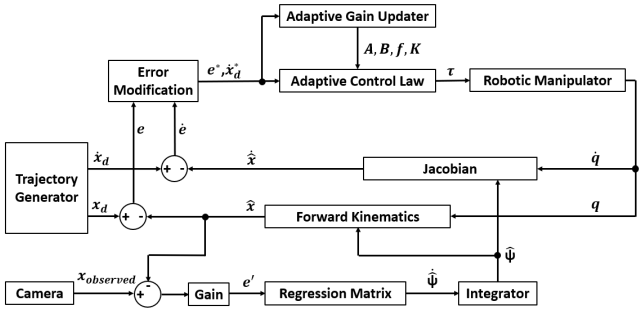

Fig. 1. The block diagram of the proposed adaptive Controller with unknown kinematics and dynamics.

Given the modified adaptive control law and the exponential stability characteristics of the exponentially stable kinematics observer, the following robust stability criterion for the adaptive control law with kinematics observer can be formulated following Theorem 1 (Colbaugh et al., 1995):

Theorem 1. The modified adaptive model-free controller (25)-(29) with kinematics observer (18) guarantees that e, e^*, f, A, B, K are globally uniformly bounded. The state error e is guaranteed to converge to a compact set that can be made arbitrarily small.

Proof. *(abbreviated)* Let us consider the following errors (similar to Colbaugh et al. (1995)) considering (3):

$$\Phi_f = f - G_c,\ \Phi_A = A - M_c,\ \Phi_B = B - V_c,\ \Phi_K = K + V_c. \tag{30}$$

The Lyapunov equation for closed-loop stability and performance analysis is

$$V = e^{*T} M_c e^* + k\lambda e^T e + \frac{1}{2\beta_1}\Phi_f^T\Phi_f + \frac{1}{2}\mathrm{tr}\left[\frac{1}{\beta_2}\Phi_A\Phi_A^T + \frac{1}{\beta_3}\Phi_B\Phi_B^T + \frac{1}{\beta_4}\Phi_K\Phi_K^T\right] \tag{31}$$

This function, V, is positive definite in $\{e^*, e, \Phi_f, \Phi_A, \Phi_B, \Phi_K\}$. The closed loop analysis is inspired by Colbaugh et al. (1995). However, here we need to look at the error terms introduced through the use of the estimated kinematics, (16) and (17). It follows from (25):

$$\tau = A(t)\ddot{x}_d^* + B(t)\dot{x}_d^* + f(t) + [2k + K(t)]e^* \\ (V_c - \Phi_B)(\lambda e') + [2k + \Phi_K - K](\dot{e}' + \lambda e') \tag{32}$$

$$\dot{f} = -\alpha_1 f + \beta_1 e^* + \underbrace{\beta_1(\dot{e}' + \lambda e')}_{=\epsilon_1} \tag{33}$$

$$\dot{A} = -\alpha_2 A + \beta_2 e^*(\ddot{x}_d^*)^T + \underbrace{\beta_2(\dot{e}' + \lambda e')(\ddot{x}_d^*)^T}_{=\epsilon_{2a}} + \underbrace{\beta_2(\dot{e}' + \lambda e')(\lambda\dot{e}')^T}_{=\epsilon_{2b}} \tag{34}$$

$$\dot{B} = -\alpha_3 B + \beta_3 e^*(\dot{x}_d^*)^T + \underbrace{\beta_3(\dot{e}' + \lambda e')(\dot{x}_d^*)^T}_{=\epsilon_{3a}} + \underbrace{\beta_3(\dot{e}' + \lambda e')(\lambda e')^T}_{=\epsilon_{3b}} \tag{35}$$

$$\dot{K} = -\alpha_4 K + \beta_4 e^*(e^*)^T + \underbrace{\beta_4(\dot{e}' + \lambda e')(e^*)^T}_{=\epsilon_{4a}} + \underbrace{\beta_4(\dot{e}' + \lambda e')(\dot{e}' + \lambda e')^T}_{=\epsilon_{4b}} \tag{36}$$

It follows that there are positive constants η_0, η_1, η_{2a}, η_{2b}, η_{3a}, η_{3b}, η_{4a} and η_{4b} so that

$$\begin{aligned}
&\|\lambda e'\| \le \eta_0 e^{-\frac{\alpha_v}{2}t} \\
&\|\epsilon_1\| \le \beta_1\eta_1 e^{-\frac{\alpha_v}{2}t} \\
&\|\epsilon_{2a}\| \le \beta_2\eta_{2a}e^{-\frac{\alpha_v}{2}t}\|\ddot{x}_d^*\|,\ \beta_2\|\epsilon_{2b}\| \le \eta_{2b}e^{-\alpha_v t} \\
&\|\epsilon_{3a}\| \le \beta_3\eta_{3a}e^{-\frac{\alpha_v}{2}t}\|\dot{x}_d^*\|,\ \ \|\epsilon_{3b}\| \le \beta_3\eta_{3b}e^{-\alpha_v t} \\
&\|\epsilon_{4a}\| \le \beta_4\eta_{4a}e^{-\frac{\alpha_v}{2}t}\|e^*\|,\ \ \|\epsilon_{4b}\| \le \beta_4\eta_{4b}e^{-\alpha_v t}
\end{aligned} \tag{37}$$

Hence, from (Colbaugh et al., 1995, Appendix A), it follows for some positive α_{10}, α_{20}, α_{30} and α_{40}, the relationship $\dot{x}_d^* = \dot{x}_d + \lambda e$ and $\ddot{x}_d^* = \ddot{x}_d + \lambda e^* - \lambda^2 e$ and Young's inequality for some sufficiently small positive constants $\tilde{\eta}_0$, $\tilde{\eta}_1$, $\tilde{\eta}_2$, $\tilde{\eta}_3$, $\tilde{\eta}_{4a}$ and $\tilde{\eta}_{4b}$:

$$\begin{aligned}
\dot{V} \le &-(\frac{k}{4} - \frac{\eta_0^2 e^{-\frac{\alpha_v}{2}t}}{4\tilde{\eta}_0} - \frac{\eta_{4a}^2 e^{-\alpha_v t}}{4\tilde{\eta}_{4a}} - \frac{\lambda^2\eta_{2a}^2 e^{-\alpha_v t}}{4\tilde{\eta}_{2b}})\|e^*\|^2 \\
&-(\frac{k\lambda^2}{4} - \frac{\eta_{3a}^2 e^{-\alpha_v t}}{4\tilde{\eta}_{3a}} - \frac{\lambda^4\eta_{2a}^2 e^{-\alpha_v t}}{4\tilde{\eta}_{2b}})\|e\|^2 \\
&-(\frac{\alpha_{10}}{4\beta_1} - \tilde{\eta}_1)\|\Phi_f\|^2 - (\frac{\alpha_{20}}{4\beta_2} - \tilde{\eta}_{2a} - \tilde{\eta}_{2b} - \tilde{\eta}_{2c})\|\Phi_A\|^2 \\
&-(\frac{\alpha_{30}}{4\beta_3} - \tilde{\eta}_{3a} - \tilde{\eta}_{3b})\|\Phi_B\|^2 - (\frac{\alpha_{40}}{4\beta_3} - \tilde{\eta}_{4a} - \tilde{\eta}_{4b})\|\Phi_K\|^2 \\
&+\frac{1}{\beta_1}\delta_1 + \frac{1}{\beta_2}\delta_2 + \frac{1}{\beta_3}\delta_3 + \frac{1}{\beta_4}\delta_4 + \frac{1}{4\tilde{\eta}_1}\eta_1^2 e^{-\alpha_v t} \\
&+\frac{1}{4\tilde{\eta}_{2c}}(\eta_{2a}\|\ddot{x}_d\|e^{-\frac{\alpha_v}{2}t} + \eta_{2b}e^{-\alpha_v t})^2 \\
&+\frac{1}{4\tilde{\eta}_{3b}}(\eta_{3a}e^{-\frac{\alpha_v}{2}t}\|\dot{x}_d\| + \eta_{3b}e^{-\alpha_v t} + \eta_0 e^{-\frac{\alpha_v}{2}t}\eta_0 e^{-\frac{\alpha_v}{2}t})^2 \\
&+\frac{1}{4\tilde{\eta}_{4b}}e^{-2\alpha_v t} + \tilde{\eta}_0\|V_c\|\eta_0 e^{-\frac{\alpha_v}{2}t} \\
&+[2k + \|V_c\|]\eta_{3a}e^{-\frac{\alpha_v}{2}t}
\end{aligned} \tag{38}$$

Lemma 1 shows that the kinematics observer converges in principle independently from the controller, assuming sufficient persistent excitation exists. Hence, it follows after a finite period of time, t, for sufficiently large gain $k > 0$ (10), sufficiently small positive scalars $\tilde{\eta}_1$, $\tilde{\eta}_{2a}$, $\tilde{\eta}_{2b}$, $\tilde{\eta}_{2c}$, $\tilde{\eta}_{3a}$, $\tilde{\eta}_{3b}$, $\tilde{\eta}_{4a}$ and $\tilde{\eta}_{4b}$ the following holds

$$\begin{aligned}
&\frac{k}{4} > \frac{\eta_0^2 e^{-\frac{\alpha_v}{2}t}}{4\tilde{\eta}_0} + \frac{\eta_{4a}^2 e^{-\alpha_v t}}{4\tilde{\eta}_{4a}} + \frac{\lambda^2\eta_{2a}^2 e^{-\alpha_v t}}{4\tilde{\eta}_{2b}}, \\
&\frac{k\lambda^2}{4} > \frac{\eta_{3a}^2 e^{-\alpha_v t}}{4\tilde{\eta}_{3a}} + \frac{\lambda^4\eta_{2a}^2 e^{-\alpha_v t}}{4\tilde{\eta}_{2b}}, \\
&\frac{\alpha_{10}}{4\beta_1} > \tilde{\eta}_1,\ \frac{\alpha_{20}}{4\beta_2} > \tilde{\eta}_{2a} + \tilde{\eta}_{2b} + \tilde{\eta}_{2c} \\
&\frac{\alpha_{30}}{4\beta_3} > \tilde{\eta}_{3a} + \tilde{\eta}_{3b},\ \frac{\alpha_{40}}{4\beta_3} > \tilde{\eta}_{4a} + \tilde{\eta}_{4b}.
\end{aligned} \tag{39}$$

Hence, it follows that the first six terms of the right hand of (38) create a sum which is negative definite (and quadrativ) in $\{e^*, e, \Phi_f, \Phi_A, \Phi_B, \Phi_K\}$. The remaining terms can be argued to remain bounded for a any time t. This follows from the fact that the demand velocity $\|\dot{x}_d\|$ and acceleration $\|\ddot{x}_d\|$ are each globally bounded at all time. Moreover, the value of V_c remains bounded for any finite time t. We now consider a large enough compact set Ω in $\{e^*, e, \Phi_f, \Phi_A, \Phi_B, \Phi_K\}$ (with 0 in its interior) which also set of all possible initial conditions. There is then a compact $\Omega_a \subset \Omega$ to which the closed loop system converges and all states remain within finite time.

At that point, all the remaining terms, specifically also the product $\|V_c\|]e^{-\frac{\alpha_v}{2}t}$ remains bounded at all time and even exponentially decreases over time. Thus, the system is ultimately bounded. The compact set to which the system converges can be made arbitrarily small by choice of δ_1, δ_2, δ_3 and δ_4 (see also Colbaugh et al. (1995)). ■

4. A PRACTICAL SIMULATION ENVIRONMENT AND SIMULATION RESULTS

This section describes the creation of a practically relevant simulation environment which is used to test the described controller. Here, we introduce various factors, e.g. sensor noise, into the simulation environment to be able to demonstrate the practical feasibility of the controller. In this work, a KUKA LBR iiwa 7 R800 (KUKA GmbH, 2019) is selected as the off-the-shelf robotic manipulator being controlled. It comes with 7 rotational joints in series allowing for 7 DOF. The manipulator model is built in Matlab Simulink using the Simscape Multibody Toolbox (MathWorks, 2019). The kinematic parameters are modelled using the robot's design specifications (KUKA GmbH, 2019). The density of the manipulator itself is assumed to be unified. Therefore, the weight of each link are assumed to be distributed according to the length of each link. The centre of mass is at the geometric center of each link. Figure 2 presents the link frames of the manipulators, as well as the multi-body model of the manipulator in the simulation.

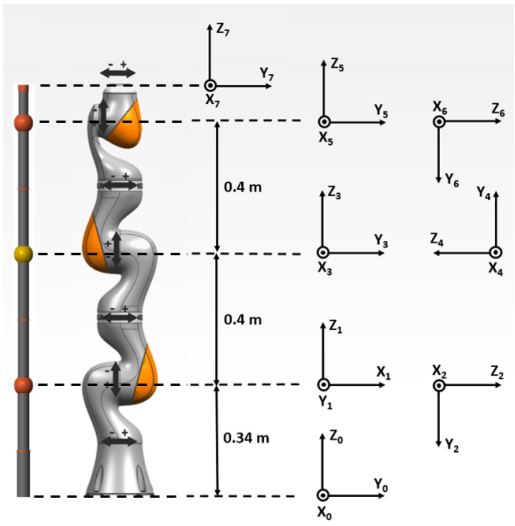

Fig. 2. A sketch of the simulated KUKA iiwa 7 R800 (middle), the assigned link frames (right), and the multi-body model in Matlab (left)

The noise from actuators and sensors are assumed to satisfy Gaussian distribution in the simulation. The assumed magnitudes of the noises are given in Table 1.

Table 1. Noise level in the simulation

Sensor/Actuator type	Standard derivation
Joint position sensor	0.001 rad
Joint torque output	0.001 Nm
Position measure via cameras	0.01 m

The dynamics of the robot's multi-body model is simulated in a continuous manner in Simulink, whereas the controller is implemented in a discretized way. Here, a sampling rate of 1 kHz is adopted as the highest sampling frequency allowing for torque control of the robot in practice (KUKA GmbH, 2019). The joint angular positions are sampled via an analogue to digital converter that are simulated by zero-order holders with 1 ms sampling period. The discrete control block outputs the control torques at each rotational joint. The torques are converted from digital to analogue signals, and the conversion is simulated using zero-order holders. In detail, the parameters in the discrete adaptive controller are configured as follows. f, A, B and K are initialized with zero elements (see equations from (25) to (29)). $\alpha_{1,2,3,4}$ are 0.001, 0.001, 0.1 and 0.001, and $\beta_{1,2,3,4}$ are set as 5, 50, 500 and 1500. λ in (24) and k in (25) are tuned as 50 and 5 respectively. Any integrator of the control system is implemented in the simulation using the Euler approximation. The continuous demand trajectory is generated using a cubic polynomial interpolation method given by Craig (2009). This strategy ensures highest smoothness for a given point-to-point movement with a specified period of time.

In the simulation environment, the manipulator is controlled to drive the tool tip to different Cartesian positions and orientations in a time period of 100s. The inertia and dimensions of the tool also change at certain time. This allows for evaluating the convergence of the kinematics observer and the overall control performance, when there is significant time-varying unknown dynamic and kinematics in the robotic system. Specifically, three situations are simulated:

(1) The target position and orientation change gradually while the kinematics remain unchanged.
(2) The kinematics parameters (tool dimensions) change gradually while the target position and orientation remain constant.
(3) The kinematics parameters (tool dimensions) change rapidly while the target position and orientation remain constant.

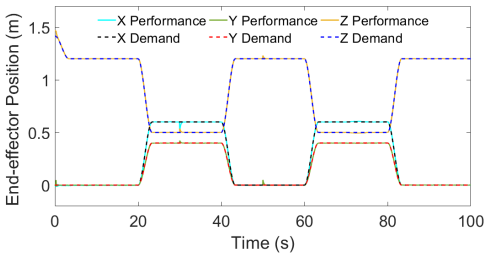

Fig. 3. Actual end-effector position against demand position

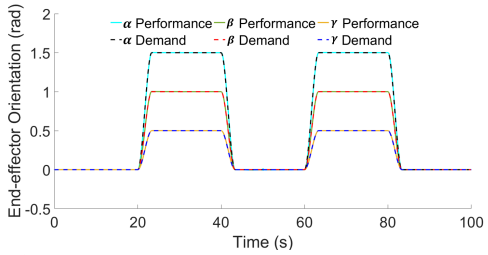

Fig. 4. Actual end-effector orientation against demand orientation. α, β, γ are the X-Y-Z Euler Angles.

In Situation 1, the end-effector is driven from a demand position (at $[0,0,1.2]^T$ m at an Euler orientation of $[0,0,0]^T$ rad) to another position (at $[0.6,0.4,0.5]^T$ m at $[1,1,1]^T$ rad Euler orientation) through a demand trajectory change in 3.3 s. During this movement, the largest error of position control is 7.8×10^{-3} m and the overshoot is 2.2×10^{-3} m. For end-effector orientation, the largest tracking error occurs in the α angle (rotation along the x-axis), with a magnitude of 1.35 $\times10^{-2}$ rad. The control for orientation has an overshoot of 2.5 $\times10^{-3}$ rad at maximum.

For the 2nd situation, the tool dimension changes gradually from $[0.04,0.1,0.18]^T$ m to $[0,0,0.2]^T$ m defined by a

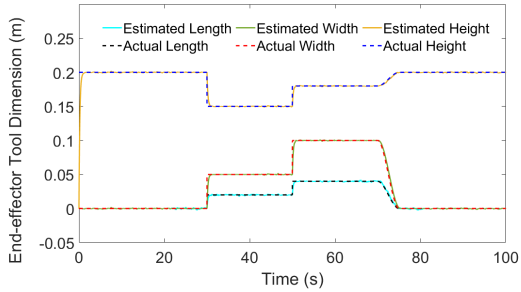

Fig. 5. Estimated dimensional information of the tool held by the manipulator.

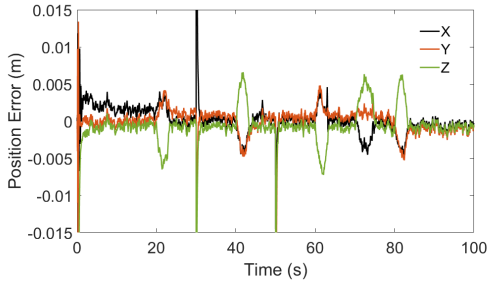

Fig. 6. Position control error of the adaptive controller.

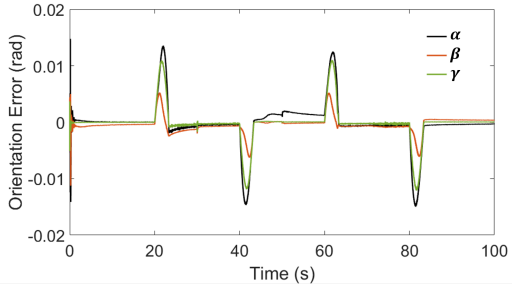

Fig. 7. Orientation control error of the adaptive controller, where α, β, γ denote the X-Y-Z Euler Angles.

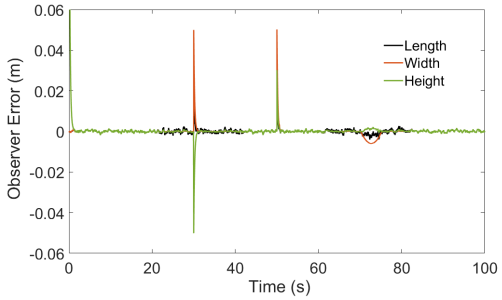

Fig. 8. Estimation error of the kinematics observer between the actual values and estimations.

cubic polynomial within an time interval of 5 s. It can be seen that the kinematics observer reacts correctly to the gradual change of the kinematics parameters, but with a time delay of 0.6 s.

The tool dimension abruptly changes from $[0,0,0.2]^T$ m (in height, width and length) to $[0.02,0.05,0.15]^T$ m in the 3rd situation. The kinematics observer takes 0.81 s to converge to the new kinematics parameters with an error less than 2×10^{-3} m.

Lastly, the steady state performance of the manipulator is investigated. The largest steady-state error is 2.1 $\times 10^{-3}$ m in position control, 4.6×10^{-4} rad in the end-effector orientation and 1.7 $\times 10^{-3}$ m in kinematics estimations.

5. CONCLUSIONS

This paper presents a new adaptive control algorithm, which compensates for unknown kinematics and dynamics online. The controller only requires the kinematic structure of the robot manipulator and achieves an accurate 3D positioning performance. The unknown dimensional information can be obtained by the developed kinematic observer. The controller is implemented for an industrial robotic manipulator in simulation. In three simulated cases, the controller shows stable and accurate performance for the end-effector control, even when the kinematics and dynamics are time-varying. A formal proof of stability has been provided (considering a scenario of piecewise constant kinematics parameters, avoiding additional complexity of a bounded temporal change in kinematics parameters).

REFERENCES

Aitken, J.M. et al. (2018). Autonomous nuclear waste management. *IEEE Intell Syst*, 33, pp.47.
Cheah, C.C. et al. (1999). Feedback control for robotic manipulator with an uncertain jacobian matrix. *J Field Robot*, 16, pp.119.
Cheah, C.C. et al. (2006). Adaptive tracking control for robots with unknown kinematic and dynamic properties. *Int J Robot Res*, 25, pp.283.
Colbaugh, R. et al. (1995). Adaptive compliant motion control for dexterous manipulators. *Int J Robot Res*, 14, pp.270.
Craig, J.J. (2009). *Introduction to robotics: mechanics and control, 3/E*. Pearson Education India.
Dixon, W.E. (2007). Adaptive regulation of amplitude limited robot manipulators with uncertain kinematics and dynamics. *IEEE T Automat Contr*, 52, pp.488.
Hsu, L. et al. (1999). Adaptive visual tracking with uncertain manipulator dynamics and uncalibrated camera. In *Proc. IEEE Conf Decis Control*, pp.1248.
KUKA GmbH (2019). KUKA robots LBR iiwa. Available from: `https://www.kuka.com/-/media/kuka-downloads/imported/48ec812b1b2947898ac2598aff70abc0/spez\_lbr\_iiwa\_en.pdf`[Accessed 22th Oct. 2019].
MathWorks (2019). Simscape multibody model and simulate multibody mechanical systems. Available from: `https://uk.mathworks.com/products/simmechanics.html`[Accessed 22th Oct. 2019].
Navarro-Alarcón, D. et al. (2013). Model-free visually servoed deformation control of elastic objects by robot manipulators. *IEEE Trans Robot*, 29, pp.1457.
Parra-Vega, V. et al. (2003). Sliding pid uncalibrated visual servoing for finite-time tracking of planar robots. In *Proc IEEE Int Conf Robot Autom*, pp.3042.
Pérez, L. et al. (2016). Robot guidance using machine vision techniques in industrial environments: A comparative review. *Sensors*.
Piepmeier, J.A. et al. (1999). A dynamic quasi-newton method for uncalibrated visual servoing. In *Proc IEEE Int Conf Robot Autom*, pp.1595.
Sastry, S. et al. (2011). *Adaptive control: stability, convergence and robustness*. Courier Corporation.
Shirai, Y. et al. (1973). Guiding a robot by visual feedback in assembling tasks. *Pattern recognition*, 5, pp.99
Siciliano, B. et al. (2010). *Robotics: modelling, planning and control*. Springer Science & Business Media.
Simoncelli, E.P. et al. (1991). Probability distributions of optical flow. In *Proc IEEE Comput Soc Conf Comput Vis Pattern Recognit*, pp.315.
Wang, H. et al. (2010). Uncalibrated visual tracking control without visual velocity. *IEEE T Contr Syst T*, 18, pp.1359.
Wang, H. et al. (2016). Visual servoing of soft robot manipulator in constrained environments with an adaptive controller. *IEEE-ASME T on Mec*, 22, pp.41.
Zergeroglu, E. et al. (2001). Vision-based nonlinear tracking controllers with uncertain robot-camera parameters. *IEEE-ASME T Mech*, 6, pp.322.